

Video-based Iris Recognition by *Quasi-Dynamic* Texture Analysis

Raissa Tavares Vieira, Virgílio de Melo Langoni, Adilson Gonzaga

Department of Electrical Engineering - EESC/USP

University of São Paulo

Av. Trabalhador São Carlense, 400

13560-590, São Carlos, SP, Brasil

raissa@ieee.org, virgilio.langoni@gmail.com, agonzaga@sc.usp.br

Abstract—In this paper, we evaluated two approaches for human iris recognition in video sequences. While applying pulses of a white led in the left eye, we have captured the iris texture in the right eye under near infrared illumination. Thus, the iris texture changes significantly during light pulse intervals. We established five time intervals according to the pupil movement. We applied a well-known method for dynamic texture analysis called LBP-TOP and we proposed to evaluate the iris texture as a sequence of frames from the same class. We have called this approach a *quasi-dynamic* method. The dynamic texture analysis captures texture information in three histograms concatenating the extracted features. The *quasi-dynamic* analysis uses the original LBP applied in video sequence as a class of static textures. The results demonstrate that our proposed methodology is better than LBP-TOP. We reached 88.6% of sensitivity and the LBP-TOP reached only 55.26%.

Keywords—*Dynamic texture; Image texture analysis; Iris recognition; Local Binary Pattern*

I. INTRODUCTION

The human iris is a highly distinctive feature of an individual to establish its identity with very high accuracy. Among all the characteristics for biometric recognition, the pattern of iris texture is one believed to be the most distinguishable among different people. The iris possesses a textural pattern due to its anatomical structure consisting of fibrous tissues, blood vessels, crypts, furrows, freckles and pigmentation. The iris texture is believed to be unique to each eye, and is thought to be stable throughout the lifespan of an individual. Thus, human recognition using the iris texture is considered to be highly reliable.

Iris recognition through still-image is covered by the most of published research studies. However, the iris recognition in video is a relatively new research subject which needs to overcome a number of challenges [1]. Challenges include recognizing a person in infrared image sequences, coping with high and low resolution, processing video sequences of people walking through a portal, matching to still face images, etc.

Iris still-images usually have noise. By using an iris video, highlights and occlusions that occur in one frame may not be present in the next. Furthermore, it is possible to obtain a better image by using multiple frames to create a better iris image [2].

Broadly speaking, still-images from iris are analyzed by ordinary static texture methods. But, considering the iris movement in video images, the texture in the frame sequences shows temporal features that could be better recognized by dynamical techniques.

The term, dynamic texture, was firstly used by Saisan et al. [3] as sequences of images that exhibit temporal stationarity. They proposed to recognizing and to classifying dynamic textures in the space of dynamical systems where each dynamic texture is uniquely represented.

More recently, Zhao and Pietikainen [4] proposed two methods for dynamic texture recognition based on the Local Binary Pattern (LBP) approach. They called one of the methods as Volume Local Binary Patterns (VLBP), which are an extension of the LBP operator, combining motion and appearance. The second proposed method was called Local Binary Patterns from Three Orthogonal Planes (LBP-TOP). In this version, they reduced the computational cost by considering only the co-occurrences of the local binary patterns on three orthogonal planes (XY-XT-YT).

The aim of this paper is to propose a method that evaluates one iris video sequence as a class of static textures varying in time. Thus, each frame is processed by the local texture analysis based on LBP. For comparison, we applied the dynamic texture model called LBP-TOP, in video sequences of iris images. We generated our own video database, by capturing the iris videos under near-infrared illumination.

The remaining of this paper is divided into five sections. In section II we show the related works about iris recognition in video images. In section III we present our proposed methodology, applying the LBP-TOP and the *quasi-dynamic* approach. The results and discussions are shown in section IV. In section V we present our conclusions.

II. IRIS IN VIDEO SEQUENCES

In 1993, Daugman [5] had already patented his method, which produces accuracy rates close to 99%. Despite the high accuracy rates, most iris recognition methods are applied to still-images.

More recently, some studies using iris video images were reported. The Video-based Automatic System for Iris Recognition (VASIR) is an iris recognition algorithm designed to work on both conventional iris images and iris images collected at a distance [1] [6]. All videos were captured while a person walked through a portal at a distance. However, video-based iris recognition at a distance is a relatively new research which still needs to overcome a number of issues.

Hollingsworth et al. [2] take advantage of the temporal continuity in an iris video to improve matching performance using signal-level fusion. From multiple frames of a frontal iris video, the authors create a single average image. Their experiments show that using average images created from ten frames of an iris video, performs better than experiments with single still-images.

Based on the eye consensual reaction, Costa and Gonzaga [7] proposed an innovative methodology to the extraction of information about the way the human eye reacts to light, and used such information for biometric recognition purposes. The results demonstrated that the proposed Dynamic Features, are discriminating, and may be employed for personal identification.

Furthermore, multiple still-images from iris have been used to improve iris recognition performance. Du [8] demonstrated higher rank on recognition rates by using three gallery images instead of one. Ma et al. [9] also enrolled three iris images and averaged the three Hamming distances to obtain the final score. Schmid et al. [10] demonstrated that fusing the scores using log likelihood ratio gave superior performance when compared to average Hamming distance. Liu and Xie [11], Roy and Bhattacharya [12] used multiple iris images for training classifiers.

Some papers were published, aiming to solve problems that occur in iris video image sequences, mainly in the “non-cooperative” or “iris-on-the-move” environment. Du et al. [13] proposed a multi-level iris video image thresholding method that takes advantage of the correlations between consecutive images for video based thresholding. The thresholded images show clear pupil and iris areas, which can help the video iris segmentation and processing. Mahadeo et al. [14] propose a technique for selecting the best frames in an iris video. Taking advantage of the temporal correspondence in iris frames, they classified iris videos in three categories, namely Adequate, Motion Constrained and Time Constrained. Zuo and Schmid [15] introduced global and local factors that can be used to evaluate iris video and image quality. The proposed measures were evaluated by analyzing the relationship between the quality of the video iris images and the system performance. These relationships indicated that the proposed quality measures influenced the recognition performance.

III. METHODOLOGY

A. Video Acquisition

For our purpose, we developed a device for the acquisition of iris image sequences, as shown in Fig. 1. This device is similar to that shown in [7], but is composed of high-performance cameras with better resolution. The left eye

receives visible light stimuli (white light) at computer-controlled specific time intervals, while the right eye image is captured and digitized into a video sequence under NIR illumination. The two sides of the device related to the left and right eye are optically isolated from each other.



Fig. 1. The proposed device to capture iris image sequences.

The video sequence obtained under NIR illumination is synchronized with the “visible light” pulses (a white LED was employed) applied to the other eye. Thus, it is possible to extract the features of the frames during pupil contraction or dilation without the interference of light reflections from the iris, pupil and sclera. Their movements are induced by the light stimulus applied to the other eye and, due to the consensual reflex, repeated by the eye whose image is being digitized without interference from visible light reflections.

The prototype was built with two multi-spectral cameras, digital and progressive scan model AD-080GE, GigE Vision compliant, belonging to the JAI C3 Advanced family [16]. The AD-080GE employs 2 CCDs, one for BAYER color and the other for NIR monochrome utilizing prism optics. The AD-080GE provides a frame rate of 30 frames/second at full resolution of 1024 (h) x 768 (v) active pixels.

In this work, we used only the right camera to capture the iris image sequence, while pulsing a white light on the left eye. We generated a database with 53 different persons and four sequences for each one taken in a random way. Some persons had their video sequences taken sequentially and others were digitized in different days. Each video sequence was established in the following way. During the video capture, we applied visible light pulses to the eye not being digitized using the white LED, whereas the camera digitizes the image sequence of the other eye that is illuminated in the near infrared band. Figure 2 shows the time intervals determined by our methodology. These intervals were defined empirically, and can be altered by the control software. Thus, each video has several frames of the iris with dilated pupil and other frames with contracted pupil.

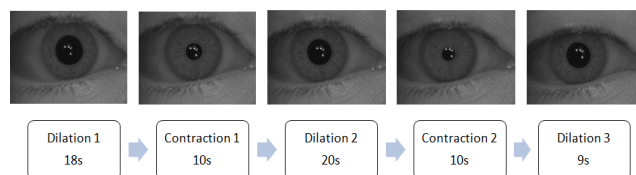


Fig. 2. Time interval during the pupil dilation and contraction.

B. Video pre-processing

In order to segment the iris, we have to exclude the regions that will interfere with the recognition, such as the eyelashes and the eyelids. Due to eye movements, it is necessary to delete those frames that cannot be used for the recognition method and select only the adequate ones. The algorithm excludes the inadequate frames and uses the remaining ones as did in [7].

We pre-processed each usable (or good) frame in order to calculate the pupil center (x_c , y_c). This is done with a low-pass filter, highlight reflections elimination, image thresholding, and morphological erosion and dilation.

We calculated the pupil radius for each frame by comparing the gray-level variations from the pupil center, through the horizontal direction. This is an estimated value, and we multiplied the radius by a factor of 1.1 to guarantee a texture sample without occlusions or highlight reflections. This value was empirically defined.

From each usable frame we extracted two texture samples of 120 x 45 pixels as shown in Fig. 3. The coordinates of this two texture samples are given by:

Left texture sample:

$$\begin{aligned} x_{1L} &= x_c - 60 & \text{and} & & y_{1L} &= y_c - 1.1 * radius \\ x_{2L} &= x_c - 60 & \text{and} & & y_{2L} &= y_c - 1.1 * radius - 45 \\ x_{3L} &= x_c + 60 & \text{and} & & y_{3L} &= y_c - 1.1 * radius - 45 \\ x_{4L} &= x_c + 60 & \text{and} & & y_{4L} &= y_c - 1.1 * radius \end{aligned}$$

Right texture sample:

$$\begin{aligned} x_{1R} &= x_c - 60 & \text{and} & & y_{1R} &= y_c + 1.1 * radius \\ x_{2R} &= x_c - 60 & \text{and} & & y_{2R} &= y_c + 1.1 * radius + 45 \\ x_{3R} &= x_c + 60 & \text{and} & & y_{3R} &= y_c + 1.1 * radius + 45 \\ x_{4R} &= x_c + 60 & \text{and} & & y_{4R} &= y_c + 1.1 * radius \end{aligned}$$

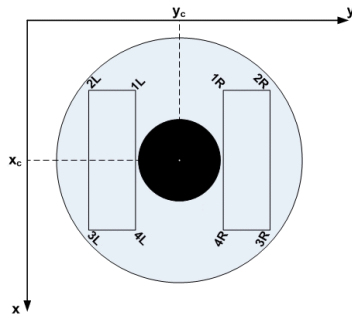


Fig. 3. Coordinates of the two texture samples.

The segmented texture samples were disposed in 10 different sets, as shown in Table I:

TABLE I. SEGMENTED TEXTURE SAMPLE SETS

LD1	Left Dilation 1
RD1	Right Dilation 1
LC1	Left Contraction 1
RC1	Right Contraction 1

LD2	Left Dilation 2
RD2	Right Dilation 2
LC2	Left Contraction 2
RC2	Right Contraction 2
LD3	Left Dilation 3
RD3	Right Dilation 3

C. Applying dynamic texture analysis based on LBP

The key problem of dynamic texture recognition is how to combine motion features with appearance features.

Zhao and Pietikainen [4] proposed to concatenate LBP on three orthogonal planes (XY, XT, and YT), considering only the co-occurrence statistics in these three directions. The video sequence is thought as a stack of XY planes in axis T, a stack of XT planes in axis Y and a stack of YT planes in axis X, respectively.

The XT and YT planes provide information about the space-time transitions. This approach was called LBP-TOP. The LBP-TOP uses three orthogonal planes that intersect in the center pixel. It considers the feature distributions from each separate plane and then concatenates them together.

The LBP code is extracted from the XY, XT, and YT planes, and denoted as XY-LBP, XT-LBP, and YT-LBP and then concatenated into a single histogram.

D. Applying local texture analysis to video frames

Our proposal for results comparison, is applying the static LBP methodology, frame by frame, in the iris video sequences. We have called this method as “quasi-dynamic”, because the involved images are sequences of video frames. Each segmented texture sample has generated a histogram with 256 bins. We used the leave-one-out cross validation comparing each histogram with the other ones.

Among several classifiers used to compute goodness of fit between two histograms, such as log-likelihood ratio and histogram intersection, we choose the Chi-square distance [17], the same metric used by [18], as the classifier (1).

$$\chi^2(P_i, Q_i) = \frac{1}{2} \sum_{i=0}^{255} \frac{(P_i - Q_i)^2}{(P_i + Q_i)} \quad (1)$$

Where, Q_i are the gray-level's frequencies of the query sample and P_i are the gray-level's frequencies of the compared sample from the set.

We generated confusion matrices with True Positives (TP), or the number of correctly classified samples, and False Negatives (FN), or the wrongly classified samples, for all of the query samples. The Hit-rate or Sensitivity was calculated by (2).

$$S = \frac{TP}{TP + FN} \quad (2)$$

Based on the texture samples extracted from each iris frame, we have established four experiments. Firstly, we selected 40 different people and two video sequences from each one. The choice was based on the best video samples with a minimal number of occlusions and reduced defocusing, avoiding twinkling. The texture samples were extracted as explained in the last section, and Table II shows the number of images used in the experiment number 01.

TABLE II. NUMBER OF IMAGES USED IN EXPERIMENT 01

	Samples from each video	Number of images
LD1	140	$140*40*2 = 11,200$
RD1	140	$140*40*2 = 11,200$
LD2	121	$121*40*2 = 9,680$
RD2	121	$121*40*2 = 9,680$
LD3	77	$77*40*2 = 6,160$
RD3	77	$77*40*2 = 6,160$
LC1	12	$12*40*2 = 960$
RC1	12	$12*40*2 = 960$
LC2	12	$12*40*2 = 960$
RC2	12	$12*40*2 = 960$

By joining the right and left textures within each interval of contraction and dilation we established the sets for the experiment number 02. By combining two regions of the segmented samples within the same side of the iris (left or right) we established the experiment number 03. In the experiment number 04, we calculated the hit-rate of one texture sample from one side (left or right) of the iris to be correctly classified, taking into account all the intervals of contraction and dilation. The sets for these experiments are shown in Table III.

TABLE III. NUMBER OF IMAGES USED IN EXPERIMENTS 02, 03, 04

Experiment 02	Number of images
D1 (LD1 + RD1)	$140*40*2*2 = 22,400$
D2 (LD2 + RD2)	$121*40*2*2 = 19,360$
D3 (LD3 + RD3)	$77*40*2*2 = 12,320$
C1 (LC1 + RC1)	$12*40*2*2 = 1,920$
C2 (LC2 + RC2)	$12*40*2*2 = 1,920$
Experiment 03	Number of images
LD12 (LD1 + LD2)	$(140+121)*40*2 = 20,880$
RD12 (RD1 + RD2)	$(140+121)*40*2 = 20,880$
LD13 (LD1 + LD3)	$(140+77)*40*2 = 17,360$
RD13 (RD1 + RD3)	$(140+77)*40*2 = 17,360$
LD23 (LD2 + LD3)	$(121+77)*40*2 = 15,840$
RD23 (RD2 + RD3)	$(121+77)*40*2 = 15,840$

LC12 (LC1 + LC2)	$(12+12)*40*2 = 1,920$
RC12 (RC1 + RC2)	$(12+12)*40*2 = 1,920$
Experiment 04	Number of images
LS (LD1 + LD2 + LD3 + LC1 + LC2)	$(140+121+77+12+12)*40*2 = 28,960$
RS (RD1 + RD2 + RD3 + RC1 + RC2)	$(140+121+77+12+12)*40*2 = 28,960$

IV. RESULTS

In this section, we show the results for each experiment explained in the last section. For each one, we calculated the correct classifications (hit-rate) and we used the chi-square distance between the query sample and the samples in each set by leave-one-out cross validation.

A. Results for the static LBP applied to sequences of video frames (quasi-dynamic)

As explained in Section III.D, we applied the texture analysis method based on the static LBP in the video frames of the acquired iris' sequences. We divided our tests in four experiments, and the achieved results for the experiment number 01 are shown in Table IV.

TABLE IV. QUASI-DYNAMIC HIT-RATE OF THE EXPERIMENT 01

	Number of Samples	Hit-rate
LD1	11,200	88.58%
RD1	11,200	82.61%
LC1	960	76.45%
RC1	960	72.91%
LD2	9,680	88.13%
RD2	9,680	83.11%
LC2	960	77.91%
RC2	960	73.75%
LD3	6,160	81.62%
RD3	6,160	82.01%

We can see that during the contraction intervals the classification performance is worse than during the dilation intervals. The best result was reached in the first interval from the left side (LD1) when the eye was not submitted to light pulses yet. During the pupil dilation intervals, at the end of the process, even with a half of samples (LD3), the hit-rate for the left textures, was reduced by 6.96%. It is interesting to observe that, in general, the left side of the iris shows a better recognition rate than the right side. When we consider the texture samples within each interval (dilation and contraction) joined together, the method performance was worse than when the texture samples were analyzed by their individual sets. The Table V shows the hit-rate calculated for the experiments 02, 03 and 04.

Considering the results obtained by the experiment number 02, we can observe that the method performance is better in the first interval, that is, when the light pulse was not applied to the person's eye. In the experiment number 03 the hit-rate shows that the best performance occurs in the first time interval by analyzing samples from the left dilation associated with samples from the same place during the second dilation.

TABLE V. QUASI-DYNAMIC HIT-RATE OF THE EXPERIMENTS 02,03,04

Experiment 02	Number of Samples	Hit-rate
D1	22,400	80.96%
C1	1,920	68.07%
D2	19,360	80.60%
C2	920	68.75%
D3	12,320	75.97%
Experiment 03	Number of Samples	Hit-rate
LD12	20,880	84.38%
RD12	20,880	78.98%
LD13	17,360	82.10%
RD13	17,360	78.01%
LD23	15,840	83.08%
RD23	15,840	80.65%
LC12	1,920	77.39%
RC12	1,920	72.55%
Experiment 04	Number of Samples	Hit-rate
LS	28,960	80.76%
RS	28,960	76.80%

Taking into account all the texture samples extracted from one side of the video sequence for all the 40 individuals, and comparing the correct classifications for the left side and for the right side, we saw in the results obtained in the experiment number 04 that the left side is more discriminant than the right side. However, the best result was achieved when we have analyzed the correct classifications given by the texture's samples extracted from the left side during the first interval of acquisition. In this time interval we have not applied a light pulse and the pupil was dilated.

Based on our tests, when we applied the LBP methodology for iris texture analysis the best results were achieved when the eye's pupil was dilated. We think that due to the iris muscles (trabeculas) more contracted, the iris texture is more homogeneous, and thus, more discriminant. Furthermore, the samples extracted from the left side have performed better than the samples from the right side of the iris. We don't have a scientific conclusion about this fact. Maybe it is related to the acquisition equipment and the eye position. It requires further investigations.

The texture samples extracted from the left side during the first time interval (LD1) compared to the set of samples from the same place and same time interval, gave the best correct classifications (88,58%). All the combinations of samples from other places and different time intervals show inferior performances.

B. Results for the LBP-TOP applied to video frames

We have chosen only the first experiment of the "quasi-dynamic" method for testing the dynamic texture based on LBP-TOP, due to achieving the best correct classifications among all. The texture samples have a concatenated histogram of three planes (XY-XT-YT) whereas the static LBP generates histograms of one single plane (XY) in the quasi-dynamic approach. We used the same sets of texture frames shown in the quasi-dynamic tests. The results are shown in Table VI.

TABLE VI. LBP-TOP HIT-RATE FOR EACH SET OF VIDEO SEQUENCES

	Number of Samples	Hit-rate
LD1	11,200	55.26%
RD1	11,200	44.74%
LC1	960	53.95%
RC1	960	43.42%
LD2	9,680	53.95%
RD2	9,680	40.79%
LC2	960	48.68%
RC2	960	32.89%
LD3	6,160	42.11%
RD3	6,160	40.79%

The graphics in the Fig. 4 shows the difference in performance, taking into account the time intervals of the pupil dilations and contractions.

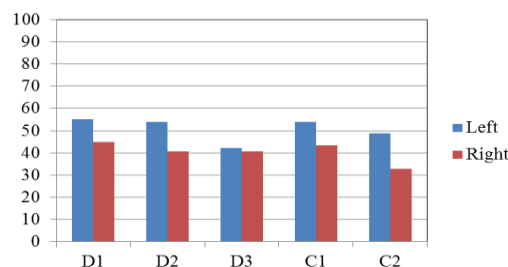


Fig. 4. Dynamic texture performance comparison to the left and right side of the iris

The proposed "quasi-dynamic" method for iris recognition by local texture analysis, by far surpassed the performance of the well-known method based on LBP-TOP. Fig. 5 shows the performance comparison between the two approaches, when the frames are considered as a video sequence within each interval of contraction and dilation.

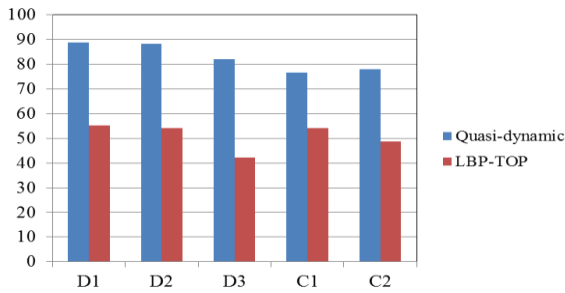


Fig. 5. Performance comparison between our proposed method and the LBP-TOP

We believe that the saccadic eye movements are the main responsible by the weak performance of the analysis based on dynamic texture. That is, the person's eye changes its position related to the camera axis, during the video acquisition. Thus, the texture variation in time, responsible to the XT and YT histogram generation, is not correlated frame by frame. Notwithstanding, the texture variations in time is not well behaved, causing the bad performance in iris recognition.

V. CONCLUSIONS

In this paper, we proposed a way of recognizing human iris, in video images with controlled pupil dilation and contraction. As we used sequence of videos, and we evaluated the local texture in each video frame during defined time intervals, we called our approach as "quasi-dynamic" methodology.

For results comparison, we applied a well known method for dynamic texture analysis. The LBP-TOP was chosen due to its similarity with our proposed approach. The difference between the two methods is that the dynamic texture analysis captures texture information in three histograms (XY-XT-YT) concatenating the extracted features. The quasi-dynamic analysis evaluates the frames in the video sequence as a class of static textures. The results demonstrate that the quasi-dynamic iris recognition, proposed by our methodology, are discriminating, and may be employed for iris identification in video sequences. The performance of our method surpasses the LBP-TOP for this application. The best hit-rate reached by our method was about 88.6% and the by the LBP-TOP was only 55.26%.

Furthermore, another interesting observation was that the samples extracted from the left side of the iris have performed better than the samples extracted from the right side. And more, we observed that the samples extracted during the first time interval, when the eye was not submitted to light pulse, have performed better than that samples extracted in time interval after light pulse application.

In addition, the possibility to extract features from living irises could increase the resistance of our approach to fraud attempts in personal identification. For example, the proposed method can check if the input image being analyzed is actually from a "living iris" or not by determining if the subject to be validated responds to the illumination stimuli applied, or if the subject is using artificial irises in an attempt to cheat the

recognition method. In addition to personal recognition, the methodology proposed also allows for the evaluation of the iris behavior at different moments under different illumination stimuli.

ACKNOWLEDGMENT

The authors would like to thank the S˜ao Paulo Research Foundation (FAPESP), grant #2011/18645-2, and National Council for Scientific and Technological Development (CNPQ) for their financial support of this research.

REFERENCES

- [1] Y. Lee, P. J. Phillips, and R. J. Micheals, "An Automated Video-Based System for Iris Recognition", in LNCS 5558, M. Tistarelli and M. S. Nixon (Eds.), ICB2009, Springer-Verlag Berlin Heidelberg 2009, pp. 1160–1169, 2009.
- [2] K. Hollingsworth, T. Peters, K. W. Bowyer, and P. J. Flynn, "Iris Recognition Using Signal-Level Fusion of Frames From Video", *IEEE Transactions on Information Forensics and Security*, vol. 4, no. 4, pp. 837–848, Dec. 2009.
- [3] P. Saisan, G. Doretto, Y. N. Wu, and S. Soatto, Dynamic Texture Recognition, in *Proc. of Conference on Computer Vision and Pattern Recognition - CVPR '01*, vol. 2, December 2001, pp. 58–63.
- [4] G. Zhao and M. Pietikainen, "Dynamic Texture Recognition Using Local Binary Patterns with an Application to Facial Expressions", *IEEE Transactions on Pattern Analysis and Machine Intelligence*, vol. 29, no. 6, June 2007, pp. 915–928.
- [5] J. Daugman, "How iris recognition works," in *Proc. Int. Conf. Image Process.*, Dec. 2002, vol. 1, pp. I-33–I-36.
- [6] Y. Lee, R. J. Micheals, J. J. Filliben, and P. J. Phillips, "Robust Iris Recognition Baseline for the Grand Challenge", National Institute of Standards and Technology, Gaithersburg, MD 20899, NISTIR 7777, March 2011.
- [7] R. M. da Costa, A. Gonzaga, "Dynamic Features for Iris Recognition, *IEEE Transactions on Systems, Man, and Cybernetics, Part B: Cybernetics*, vol. 42, no. 4, pp. 1072 – 1082, Aug. 2012
- [8] Y. Du, "Using 2D log-Gabor spatial filters for iris recognition," *SPIE Biometric Technology for Human Identification III*, vol. 62020, 2006.
- [9] L. Ma, T. Tan, Y. Wang, and D. Zhang, "Efficient iris recognition by characterizing key local variations," *IEEE Transactions on Image Processing*, vol. 13, no. 6, pp. 739–750, 2004.
- [10] N. A. Schmid, M. V. Ketkar, H. Singh, and B. Cukic, "Performance analysis of iris based identification system at the matching score level," *IEEE Transactions on Information Forensics and Security*, vol. 1, no. 2, pp. 154–168, 2006.
- [11] C. Liu and M. Xie, "Iris recognition based on DLDA," in *Proc. International Conference on Pattern Recognition*, pp. 489–492, 2006.
- [12] K. Roy and P. Bhattacharya, "Iris recognition with support vector machines," in *Proc. International Conference on Biometrics*, pp. 486–492, 2006.
- [13] Y. Du, N. L. Thomas, and E. Arslanturk, "Multi-level Iris Video Image Thresholding", *IEEE Workshop on Computational Intelligence in Biometrics: Theory, Algorithms, and Applications, CIB 2009*, pp. 38 – 45, 2009.
- [14] N. K. Mahadeo, A. P. Paplinski, S. Ray, "Automated Selection of Optimal Frames in NIR Iris Videos", in *Proc. of 2013 International Conference on Digital Image Computing: Techniques and Applications (DICTA)*, Hobart, TAS, 26–28 Nov., pp.1 – 8, 2013.
- [15] J. Zuo and N. A. Schmid, "Global and Local Quality Measures for NIR Iris Video", in *Proc. of IEEE Computer Society Conference on Computer Vision and Pattern Recognition Workshops, CVPR Workshops*, Miami, FL, 20–25 June, pp.120–125, 2009.
- [16] JAI – AD-080GE camera: <http://www.jai.com/en/products/ad-080ge>
- [17] M. W. O. Pele, "The quadratic-chi histogram distance family". in *Proc. of the 11th European conference on Computer vision Part II (ECCV'10)*, Berlin, Heidelberg, 2010. Springer-Verlag, pp. 749–762.
Z. Guo, L. Zhang, D. Zhang, "A completed modeling of local binary pattern operator for texture classification", *IEEE Transactions on Image Processing*, vol. 19, Issue 6, June 2010.